## Crucial Mitochondrial Impairment upon CDC48 Mutation in **Apoptotic Yeast\***

Received for publication, December 23, 2005, and in revised form, April 6, 2006 Published, JBC Papers in Press, July 5, 2006, DOI 10.1074/jbc.M513699200

Ralf J. Braun<sup>‡1</sup>, Hans Zischka<sup>‡§1,2</sup>, Frank Madeo<sup>¶</sup>, Tobias Eisenberg<sup>¶</sup>, Silke Wissing<sup>||</sup>, Sabrina Büttner<sup>¶</sup>, Silvia M. Engelhardt<sup>||</sup>, Dietmute Büringer\*\*, and Marius Ueffing<sup>‡ ‡</sup>

From the  $^{\dagger}$ GSF-National Research Center for Environment and Health, Institute of Human Genetics, Ingolstaedter Landstrasse 1, Munich-Neuherberg D-85764, Germany, the §GSF-National Research Center for Environment and Health, Institute of Toxicology, Munich-Neuherberg D-85764, Germany, the University of Graz, Institute of Molecular Biosciences, Graz A-8010, Austria, the  $^{\parallel}$ University of Tübingen, Institute for Physiological Chemistry, Tübingen D-72076, Germany, the \*\*Max Planck Institute for Neurobiology, Department of Systems and Computational Neurobiology, Martinsried D-82152, Germany, and the  $^{\ddagger +}$ Technical University Munich, Institute of Human Genetics, Klinikum rechts der Isar, Munich D-81675, Germany

Mutation in CDC48 (cdc48<sup>S565G</sup>), a gene essential in the endoplasmic reticulum (ER)-associated protein degradation (ERAD) pathway, led to the discovery of apoptosis as a mechanism of cell death in the unicellular organism Saccharomyces cerevisiae. Elucidating Cdc48p-mediated apoptosis in yeast is of particular interest, because Cdc48p is the highly conserved yeast orthologue of human valosin-containing protein (VCP), a pathological effector for polyglutamine disorders and myopathies. Here we show distinct proteomic alterations in mitochondria in the cdc48<sup>S565G</sup> yeast strain. These observed molecular alterations can be related to functional impairment of these organelles as suggested by respiratory deficiency of cdc48<sup>S565G</sup> cells. Mitochondrial dysfunction in the  $cdc48^{\mathrm{S565G}}$  strain is accompanied by structural damage of mitochondria indicated by the accumulation of cytochrome c in the cytosol and mitochondrial enlargement. We demonstrate accumulation of reactive oxygen species produced predominantly by the cytochrome  $bc_1$  complex of the mitochondrial respiratory chain as suggested by the use of inhibitors of this complex. Concomitantly, emergence of caspase-like enzymatic activity occurs suggesting a role for caspases in the cell death process. These data strongly point for the first time to a mitochondrial involvement in Cdc48p/VCPdependent apoptosis.

Fundamental cellular processes, such as the formation of organelles (ER,3 Golgi apparatus, and the nuclear envelope), or

ubiquitin-dependent ER-associated protein degradation (ERAD) have been linked to the yeast protein Cdc48p and its highly conserved mammalian orthologue VCP (1-4). Mutations in VCP have been associated with "inclusion body myopathy associated with Paget disease of bone and frontotemporal dementia" (IBMPFD), a dominant human disorder (5, 6). A genetic screening of a Drosophila model for human polyglutamine diseases, a class of inherited neurodegenerative disorders, identified the *Drosophila* homologue of Cdc48p/VCP as a modulator of apoptotic cell death (7), leading these authors to propose VCP as a pathological effector for polyglutamine-induced neurodegeneration. However, the cellular mechanisms underlying VCP-mediated cell death in these human disorders remain largely unknown.

Apoptotic phenotypes in cells expressing mutated Cdc48p/ VCP have originally been described in budding yeast (8) and were thereafter confirmed in mammalian cell cultures (9, 10), in trypanosomes (11), and in zebrafish (12). Notably, Cdc48p was the first apoptotic mediator found in Saccharomyces cerevisiae (8). The expression of a point-mutated CDC48 gene (cdc48<sup>S565G</sup>) leads to a characteristic apoptotic phenotype: phosphatidylserine externalization, DNA fragmentation, chromatin condensation, nuclear fragmentation, and vacuolization (8, 13). These results obtained in the  $cdc48^{S565G}$  strain initiated the establishment of yeast as a model to study evolutionary conserved mechanisms of apoptotic regulation (14-16).

Mitochondria play a crucial role in many apoptotic pathways in both mammalian cells and in yeast (17–19). In the present study, we therefore tested for mitochondrial impairment and contribution in Cdc48p-mediated apoptosis. We observed mitochondrial enlargement, distinct alterations in the mitochondrial proteome, release of cytochrome *c* into the cytosol, impairment in the ability of  $cdc48^{S565G}$  cells to adapt to respiratory conditions, as well as mitochondrial ROS production

with Paget disease of bone and frontotemporal dementia; VCP, valosincontaining protein; EM, electron microscopy; 2-DE, two-dimensional gel electrophoresis; MALDI-TOF, matrix-assisted laser desorption ionization time-of-flight; ROS, reactive oxygen species; PBS, phosphate-buffered saline; FITC, fluorescein isothiocyanate; FMK, fluoromethyl ketone; TUNEL, terminal deoxynucleotidyl transferase-mediated dUTP nick end labeling; MMF1, maintenance of mitochondrial function 1; MRP8, mitochondrial 40 S ribosomal protein; NE, nuclear envelope; T, total percentage concentration of acrylamide and bisacrylamide monomers.



<sup>\*</sup> This work was supported by the German Federal Ministry for Education and Research (Grant FKZ 031U108E, subproject B3 to H. Z., R. J. B., and M. U.), NGFN2 SMP Proteomics (Grant FKZ 01GR0449, subproject 9 to R. J. B. and M. U.), the European Union EU-IP "Interaction Proteome" (Grant LSHG-CT-2003-505520 to R. J. B. and M. U.), the Deutsche Forschungsgemeinschaft (to F. M., S. M. E., and S. W.), and the Austrian "Fonds zur Förderung der wissenschaftlichen Forschung" Project (Grant S9304-B05 to F. M., T. E., and S. B.) The costs of publication of this article were defrayed in part by the payment of page charges. This article must therefore be hereby marked "advertisement" in accordance with 18 U.S.C. Section 1734 solely to indicate this fact.

The on-line version of this article (available at http://www.jbc.org) contains supplemental Fig. S1.

<sup>&</sup>lt;sup>1</sup> Both authors contributed equally to this work.

<sup>&</sup>lt;sup>2</sup> To whom correspondence should be addressed. Tel.: 49(0)89-3187-2663; Fax: 49(0)89-3187-3449; E-mail: zischka@gsf.de.

<sup>&</sup>lt;sup>3</sup> The abbreviations used are: ER, endoplasmic reticulum; ERAD, ER-associated protein degradation; IBMPFD, inclusion body myopathy associated

### Mitochondrial Impairment in cdc48<sup>S565G</sup> Yeast

paralleled to the emergence of caspase-like enzymatic activity. These data show mitochondrial impairment at morphological, molecular, and functional levels. These alterations are associated with apoptotic cell death indicating the activation of a mitochondrial pathway for Cdc48p-mediated apoptosis.

### **EXPERIMENTAL PROCEDURES**

Yeast Strains, Culture Conditions, and Assay for Respiratory Deficiency—S. cerevisiae wild-type KFY417 (CDC48) and mutant strain KFY437 (cdc48<sup>S565G</sup>) (20) were used in this study. For all experiments (except  $\rho^0/\rho^+$  experiments, see below) induction of apoptosis was done as follows (8, 13): glucose medium (YP medium, 1% yeast extract, 2% Bacto Peptone, supplemented with 4% glucose, Otto Nordwald, Hamburg, Germany) was inoculated ( $A_{600} = 0.1-0.3$ ) with stationary YPGal pre-cultures (YP medium supplemented with 4% galactose). Cells were then grown in baffled flasks at 28 °C until early stationary and stationary phases, respectively, and then subjected to heat shock at 37 °C.

For analysis of respiratory deficiency, glucose cultures of both wild-type and *cdc*48<sup>S565G</sup> strains were plated on YP plates (YP medium supplemented with 1.5% agar) containing (i) 4% glucose (YPGlc, fermentative selective medium) or (ii) 2% lactate (YPLac, respiratory selective medium). Cultures were spotted on agar plates in dilution series (from  $5 \times 10^6$  cells to  $5 \times$ 10<sup>1</sup> cells in 10-fold dilution steps) clockwise on six distinct sections. After 5 days of incubation at room temperature, the sections were evaluated for growth.

 $\rho^0$  strains (yeast strains lacking functional mitochondria) were generated from the respective  $\rho^+$  strains (KFY417 and KFY437) by growing cells in media containing 10  $\mu$ g/ml ethidium bromide for 3 days. The resulting respiratory deficiency was confirmed by complete lack of growth on obligatory respiratory media (glycerol). In  $\rho^0/\rho^+$  experiments, cells were grown and treated as described for KFY417 and KFY437 (see above) with the modification that pre-cultures were grown in YPGal/Glc (3% galactose/1% glucose), because the generated  $\rho^0$ strains were unable to grow in YPGal.

*Electron Microscopy*—EM analysis of mitochondrial samples was carried out as previously described (21). EM analysis of stationary yeast cells to visualize membrane structures was done essentially according to Ref. 22: cells were harvested and incubated for 8 min in fixative (4% formaldehyde, 2% glutaraldehyde, 4% sucrose, 2 mm calcium acetate, 50 mm sodium cacodylate, pH 7.2) at room temperature. Fixed cells were stored in fixative overnight at 4 °C and subsequently prepared for cell wall removal by incubation in pretreatment solution (0.2 M Tris/HCl, 100 mM β-mercaptoethanol) for 10 min at room temperature. Removal of cell wall was done with 30 units of lyticase (Sigma) and 0.6 unit of arylsulfatase (Roche Applied Science) for 90 min at 30 °C in digestion buffer (35 mm potassium phosphate buffer, pH 6.8, 0.5 mm MgCl<sub>2</sub>, 1.2 m sorbitol). Cells were washed in cacodylate buffer (0.1 M sodium cacodylate, 5 mm CaCl<sub>2</sub>), postfixed (0.5% osmium tetroxide, 0.8% potassium ferrocyanide), washed in distilled water, stained en bloc (1% aqueous uranyl acetate), dehydrated in ascending alcohol series, and embedded in Araldite. The preparations were sectioned at 50 nm on an ultramicrotome (Ultrotom III, LKB, Bromma,

Sweden), and EM micrographs were obtained on a Zeiss (Oberkochen, Germany) EM 10 electron microscope.

Cell Fractionation—Mitochondria were isolated by differential centrifugation as described in Zischka et al. (21). Cytosol was obtained by ultracentrifugation (177,000  $\times$  g, 90 min, 4 °C) from the supernatant of the first mitochondrial sedimentation.

Two-dimensional Gel Electrophoresis and Image Analysis— 2-DE was performed according to Zischka et al. (21). Isoelectric focusing was done using immobilized pH-gradient strips (pH 3-10 non-linear) and gradient gels (8-16% T) for SDS-PAGE. Resultant protein patterns were detected by standard staining procedures, either silver (23) for analytical purposes (150  $\mu g$  of protein per gel) or "ruthenium II Tris bathophenanthroline disulfonate fluorescent dye" (24) for preparative purposes (400 μg of protein per gel). Gels treated with the latter were further stained with colloidal Coomassie Blue for protein analysis (25). Image analysis of the gels was done with the ProteomWeaver  $^{\mathrm{TM}}$ image analysis software V.2.2 (Definiens AG, Munich, Germany). For the analysis of mitochondrial extracts data were determined by taking into account three independent experiments.

Protein Identification via MALDI-TOF Mass Spectrometry-Proteins were subjected to a sequence-dependent protease treatment (100 ng of trypsin per gel plug, Promega, Mannheim, Germany) as described by Shevchenko et al. (23). Resulting peptides were analyzed by peptide mass fingerprinting with the thin layer method (26) using a MALDI-TOF Reflectron (Waters, Eschborn, Germany). Data base searches for protein identification were done in SwissProt using the ProteinLynx Globalserver 1.1 software (PLGS 1.1, Waters).

SDS-PAGE and Immunoblotting Analysis—SDS-PAGE and subsequent immunoblotting on polyvinylidene difluoride membranes were carried out according to standard procedures. Immunoblots were incubated with anti-55 kDa cytosolic protein (kind gift of G. Blobel) and anti-cytochrome c (kind gift of F. Sherman), respectively. Immunoreactive bands were visualized by ECL plus (GE Healthcare, Freiburg, Germany) and quantified using QuantityOne® V.4.2 software (Bio-Rad, Munich, Germany).

Staining for Reactive Oxygen Species-ROS were detected with dihydrorhodamine 123 (Sigma) according to Madeo et al. (13) with 30-min staining at 30 °C. Cells were embedded in 0.5% agarose in PBS and evaluated for staining by fluorescence microscopy using a rhodamine optical filter (room temperature, 40×/0.75, Axioskop 2, AxioCam HRc, AxioVision 4, Zeiss, Göttingen, Germany). In  $\rho^0/\rho^+$  experiments, ROS were detected with the mitochondrial membrane potential-independent stain dihydroethidium (Sigma).  $5 \times 10^6$  cells were pelleted in 96-well microtiter plates (Microlon Fluorotrac 600, Greiner, Austria), washed twice with PBS, resuspended in 250  $\mu$ l of 2.5 μg/ml dihydroethidium in PBS, and incubated for 10 min at room temperature. Relative fluorescence units were determined using a fluorescence reader (GENios Pro<sup>TM</sup>, Tecan, Grödig, Austria, excitation 515 nm, emission 595 nm, room temperature). Dihydroethidium was used as the blank in PBS. Additionally, cells were evaluated for staining by fluorescence microscopy using a rhodamine optical filter.



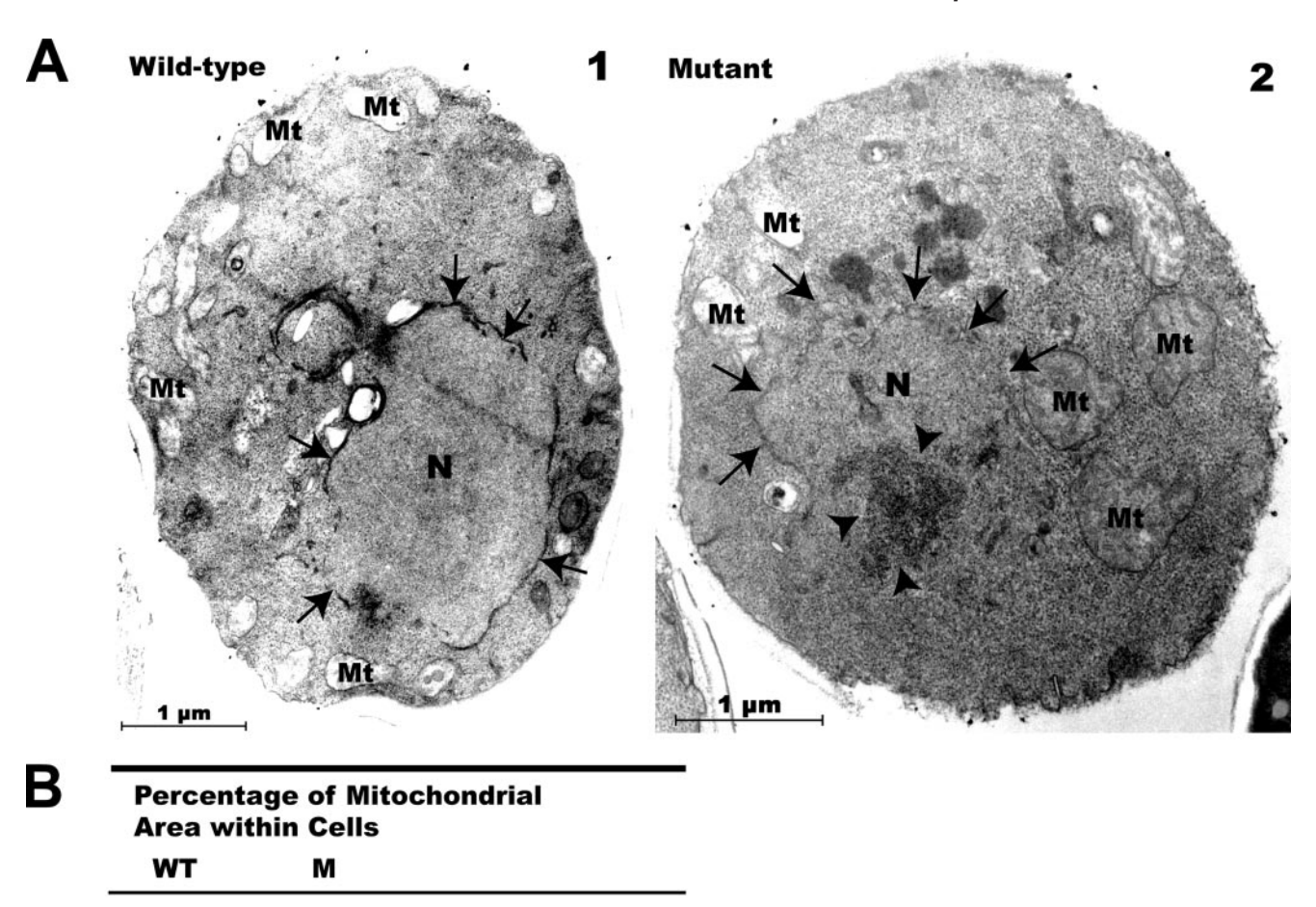


FIGURE 1. **Mitochondria are enlarged in** *cdc48*<sup>S565G</sup> **cells.** *A*, EM analysis of wild-type and *cdc48*<sup>S565G</sup> cells. Wild-type cells (1) show intact nuclei (*arrows*, nuclear envelope) with mitochondria predominantly distributed near the plasma membrane. *Cdc48*<sup>S565G</sup> cells (2) frequently demonstrate chromatin condensations. sation (arrowheads), nuclear fragmentation, and enlarged mitochondria. Mt, mitochondria; N, nucleus; arrows, nuclear envelope; arrowheads, chromatin condensation. B, quantification of mitochondrial enlargement. Mitochondrial and total cellular area was determined using AxioVision Software LE V.4.2 (Zeiss). To exclude artifacts due to the fixation procedure, mitochondrial area was normalized to total cellular area. The obtained percentage of the mitochondrial area within cells was significantly increased in  $cdc48^{SS6SG}$  (10%) compared with wild-type cells (7%) (p < 0.02, Student's t test). These figures represent enlargement of mitochondria in  $cdc48^{SS6SG}$  cells, because the average number of mitochondria within 1  $\mu$ m<sup>2</sup> of cellular area remained unchanged (1.1 for wild-type and 1.2 for  $cdc48^{SS6SG}$  cells). For quantification and statistics 62 and 128 mitochondria for wild-type and  $cdc48^{SS6SG}$  strain, respectively, were evaluated.

Survival Plating Assay—Survival plating assays were done as previously described (27). Briefly, an aliquot of the culture was counted with a CASY1 (Schärfe Systems, Reutlingen, Germany), diluted 1:10,000 in water, and 500 cells were plated on YPGlc plates (4% glucose). The number of colonies (colony forming units) was determined after incubating the plates for 2–3 days at 28 °C. For each experiment three plates per strain and condition were evaluated for growth of colonies.

10%

2%

**StDev** 

Student's t-Test

Tests for Apoptotic Markers—In vivo measurement of caspaselike enzymatic activity by flow cytometric analysis was done as previously described (27). Briefly, cells were harvested, washed in PBS, and resuspended in staining solution containing fluorescein isothiocyanate (FITC)-VAD-FMK (CaspACE<sup>TM</sup>, Promega). After incubation for 20 min at 30 °C, cells were washed and resuspended in PBS. Stained cells were counted using a FACSCalibur (BD Biosciences) and Cell Quest analysis software. CaspACE<sup>TM</sup> FITC-VAD-FMK in situ marker is an FITC conjugate of the cell-permeable caspase inhibitor VAD-FMK. This structure allows delivery of the inhibitor into the cell where it binds to activated caspase, serving as an in situ marker for apoptosis. The bound marker is localized by fluorescence detection.

The T4 terminal deoxynucleotidyl transferase-mediated dUTP nick end labeling (TUNEL) assay was used to visualize DNA fragmentation, a late marker of apoptosis. Cell wall digestion and cell fixation were done as described by Madeo et al. (8). TUNEL reaction was performed using an in situ cell death detection kit (Roche Applied Science) and Chromatide Bodipy<sup>TM</sup> (Molecular Probes, Invitrogen, Karlsruhe, Germany) as fluorescence-labeled dUTP. Cells were evaluated for stained nuclei by fluorescence microscopy using a FITC optical filter (room temperature, 40×/0.75, Axioskop 2, AxioCam HRc, AxioVision 4).

7%

1%

p = 0.02

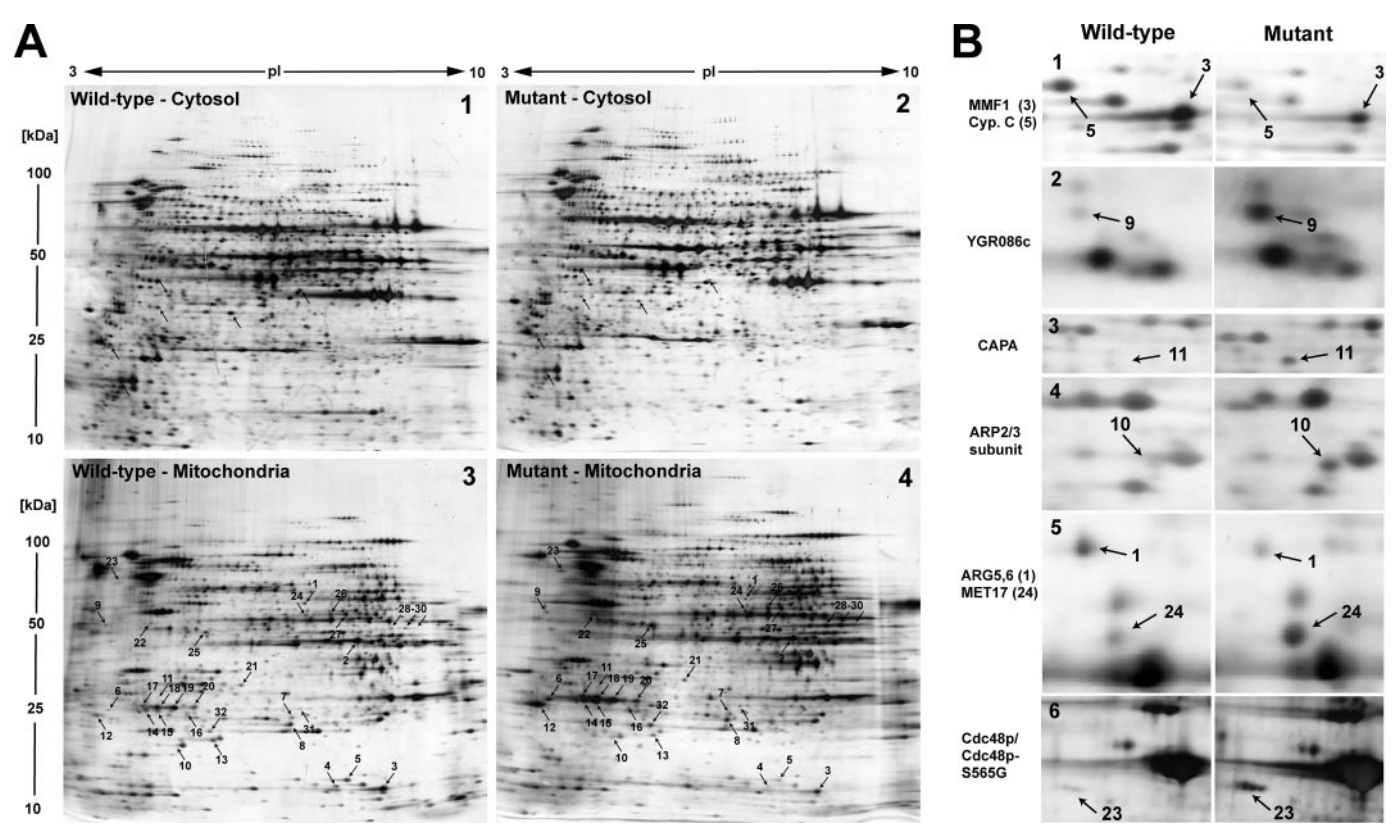


FIGURE 2. **Differential 2-DE analysis of mitochondrial and cytosolic fractions from wild-type and** *cdc48*<sup>5565G</sup> **cells.** *A*, 2-DE comparison of cytosolic extracts (wild-type versus cdc48<sup>5565G</sup>, gels 1 and 2, respectively): 6 reproducible differences (*arrows*) out of 1600 protein spots per gel were found (Proteom Weaver<sup>TM</sup>) (n = 6). Comparison of mitochondrial extracts (gels 3 and 4): 32 reproducible differences (arrows) out of 1400 protein spots per gel were found; identified proteins and results of quantification (ProteomWeaver<sup>TM</sup>) are listed in Table 1 (n = 7). B, representative differences between wild-type and  $cdc48^{S56SG}$  strains in mitochondrial extracts.

### **RESULTS**

Mitochondria in cdc48<sup>SS65G</sup> Cells Are Enlarged Compared with Wild-type—To check for mitochondrial impairment in the apoptotic  $cdc48^{S565G}$  yeast strain we performed ultrastructural analysis (EM) of yeast cells. In cdc48S565G cells we observed a significant enlargement of mitochondria compared with wild type (Fig. 1A, for quantification see Fig. 1B). In the cdc48<sup>S565G</sup> strain 10% of the cellular area was composed of mitochondria compared with 7% in the wild-type strain. Because the average number of mitochondria per cell was highly similar between the cdc48<sup>S565G</sup> and wild-type strains (1.1 for wild-type and 1.2 for cdc48<sup>SS65G</sup> cells), these data hint toward a swelling of mitochondria in the cdc48<sup>S565G</sup> strain, which is a known feature in pathophysiological processes (28-31).

Distinct Alterations Are Observed in the Mitochondrial Proteome of cdc48<sup>SS6SG</sup> Cells Compared with Wild-type—We further investigated whether mitochondrial enlargement in the cdc48S565G strain was concomitant with alterations at the molecular level of mitochondria. Therefore, we analyzed the mitochondrial proteome applying differential 2-DE analysis of wild-type and cdc48S565G strains. Additionally, we compared their total cell extracts and their cytosolic proteomes.

Differential 2-DE analysis of mitochondria resulted in 32 significant protein spot variations between wild-type and cdc48<sup>S565G</sup> strains (Fig. 2A, compare gels 3 and 4, and Table 1). In contrast, only minimal differences were observed in cytosolic fractions (Fig. 2A, compare gels 1 and 2), and the overall cellular proteome remained unchanged (data not shown).

Mass spectrometry analysis of the 32 altered protein spots in mitochondria identified 23 unique proteins (Table 1), seven of which were established as mitochondrial proteins. Increased ("enrichment") and decreased ("depletion") amounts of mitochondrial proteins in mitochondrial extracts of cdc48<sup>S565G</sup> cells were observed (e.g. YGR086c (Fig. 2B, panel 2) and maintenance of mitochondrial function 1 (MMF1, Fig. 2B, panel 1), respectively; for quantification of protein spot alterations see Table 1).

The observed depletion of MMF1 (Fig. 2B, panel 1) and ketol acid reductoisomerase (Ilv5p, Table 1), two mitochondrial proteins fundamental for the stability of mitochondrial DNA (32, 33), suggest reduced mitochondrial functionality upon CDC48 mutation. We found depletion of mitochondrial cyclophilin C (Fig. 2B, panel 1) and enrichment of mitochondrial 40 S ribosomal protein (MRP8) (Table 1) in mitochondrial extracts. Cyclophilins are enzymes that catalyze cis-trans isomerization of proline-containing peptides to ensure accurate protein folding (34). MRP8 is a component of the mitochondrial protein translation machinery (35). Alterations in the amount of cyclophilin C and MRP8 therefore may suggest an altered protein turnover in mitochondria. Discrete changes of mitochondrial proteins in mitochondrial extracts suggest that mitochondria are altered upon CDC48 mutation possibly leading to mitochondrial dysfunction.

# Identified proteins differentially found in mitochondrial extracts

For MALDI-TOF mass spectrometry, protein spots were subjected to trypsin treatment. Resulting peptides were analyzed by peptide mass fingerprinting using a MALDI-TOF Reflectron (Waters). Spectra were annotated applying MassLynx software (Waters), Subsequent data base searches in SwissProt were done using the ProteinLynx Globalserver 1.1 software (PLGS 1.1, Waters) with the following search parameters: organisms, unrestricted; peptide mass, unrestricted; peptide mass undifications, oxidations (M); mass values, monoisotopic; protein mass, unrestricted; peptide mass tolerance, ±150 ppm; peptide charge state, 1+; maximum missed cleavages, 1. For the analysis of mitochondrial extracts data were determined by taking in account three independent experiments. In total seven two-dimensional gels for wild-type and seven two-dimensional gels for cdc48<sup>256,566</sup> were considered for quantification and statistics.

Spot no. (Fig. 3)	SwissProt Accession no."	Sequence	PLGS 1.1 score of identified protein/score of next yeast hit <sup>b</sup>	Matched mass values	Gene name (MIPS) <sup>c</sup>	Protein name	Relative protein spot intensities on 2-DE (cdc48 <sup>5565G</sup> versus wild type) <sup>d</sup>	p values of 2-DE image analysis (Student's t test)	Localization (Mitop2)°	Function
		%								
1 2	Q01217 P06168	42 96	54/26 201/57	9/13 13/13	YER069w YLR355c	ARG5, 6 protein Ketol acid reductoisomerase	0.5	0.00200	Mitochondria, matrix Mitochondria	Amino acid metabolism Amino acid metabolism
	5	o o	ò	2	10	(Ilv5p)		7,000		
λ, η 4,	P40185	82	82/-	6//	YILU51C	MMF1	0.4	0.00361	Mitochondria, matrix	Amino acid metabolism
n <b>v</b>	P35719	C 4	32/34	3/6	YKI.142w	MRP8	7.0	0.01214	Mitochondria	Protein biosynthesis
7,8	P08067	78	74/47	9/17	YEL024w	Ubiquinol-cytochrome $c$ reductase iron-sulfur subunit	0.65/1.2	0.04284/0.17448	Mitochondria, inner mitochondrial	Energy metabolism
						(UCRI)			membrane	
6	P53252	69	21/3	4/6	YGR086c	Hypothetical protein YGR086c/ sphingolipid long-chain base-responsive protein PIL1	3.5	0.00007	Mitochondria <sup>r</sup> , lipid particles	Membrane traffic
10	P33204	78	28/10	3/6	YKL013c	ARP2/3 complex 20-kDa subunit	3.5	0.00038	Cytoskeleton	Mitochondrial motility
11	P28495	35	31/12	7/10	YKL007w	F-actin capping protein $\alpha$ subunit (CAPA)	2.8	0.00020	Cytoskeleton	Actin cytoskeleton
12	P35691	49	13/12	3/7	YKL056c	Translationally controlled tumor protein homolog (TCTP)/ microtubule and mitochondria interacting protein (Mmilu)*	3,3	0.00037	Cytoskeleton, mitochondria- associated <sup>g</sup>	Microtubule-associated, translocates to mitochondria upon oxidative stress <sup>g</sup>
13	P39742	7,5	11/7	2/5	VI R2926	Translocation protein Sec72n	1.8	0.00460	ER membrane	Secretory nathway
14, 15	P07283	49	46/-	6/19	YFL045c	Phosphomannomutase Sec53p	1.8	0.00014	ER-associated <sup>n</sup>	Secretory pathway
16	P35176	75	22/-1	7/13	YDR304c	Cyclophilin D	0.5	0.00291	ER lumen	Protein folding
1/-20 21	P15992 P38011	69	0/-6 0/-6	6/8 4/10	YMR116c	Heat shock protein 26 (HSp.26) Guanine nucleotide-binding protein subunit beta-like	2.1	0.00106	Nucleus, cytopiasm Ribosome <sup>i</sup>	Stress response Protein biosynthesis
22	P10081	71	70/22	8/9	YKR059w	Eukaryotic initiation factor 4A	1.6	0.05509	Ribosome <sup>i</sup>	Protein biosynthesis
23	P25694	20	29/3	6/9	YDL126c	Cell division cycle protein 48 (Cdc48p)	5.8	0.00002	ER-associated, nucleus, cytosol	ERAD, organelle formation, spindle
24	P06106	09	32/8	9/20	YLR303w	O-Acetylhomoserine sulfhydrolase (MET17)	1.5	0.00630	Cytoplasm	Amino acid metabolism
25	P04173	41	48/16	8/15	YCL018w	3-Isopropylmalate dehydrogenase	1.4	0.00615	Cytoplasm	Amino acid metabolism
26, 27	P00924	57	23/-2	10/14	YGR254w	Enolase 1	2.2	0.00199	Cytoplasm	Energy metabolism
28-30	P38219	70	27/1	6/9	YBR025c	Putative GTP-binding protein	2.4	0.00803	Cytoplasm	Unknown
31	Q05016	9 <u>/</u>	22/-6	6/9	YMR226c	Putative oxidoreductase	2.8	0.01019	Unknown	Unknown
32	Q12447	ç/,	38/20	8/9	YDR0/1c	Hypothetical protein YDR0/1c	3.2	0.00070	Unknown	Unknown
"SWISSP.	data base: 11S.	" SwissProt data base: us.expasy.org/sprot/	ot/.							

<sup>&#</sup>x27; SwissProt data base: us.expasy.org/sprot/. ' PLGS 1.1 scoring. ' MIPS database: mips.gsf.de/projects/fungi.

 $<sup>^{1}</sup>$  Factor: mutant ( $cdc48^{85656}$ ) versus wild-type strain: <1 for depletion, >1 for accumulation of protein. Mitop2 data base: ihg gsf.de/mitop2/start.jsp. According to Ref. 54, high probability for mitochondrial localization according to Mitop2 data base.

According to Ref. 55. According to Ref. 56.

Ribosomal proteins are predominantly NE-ER-associated (57)

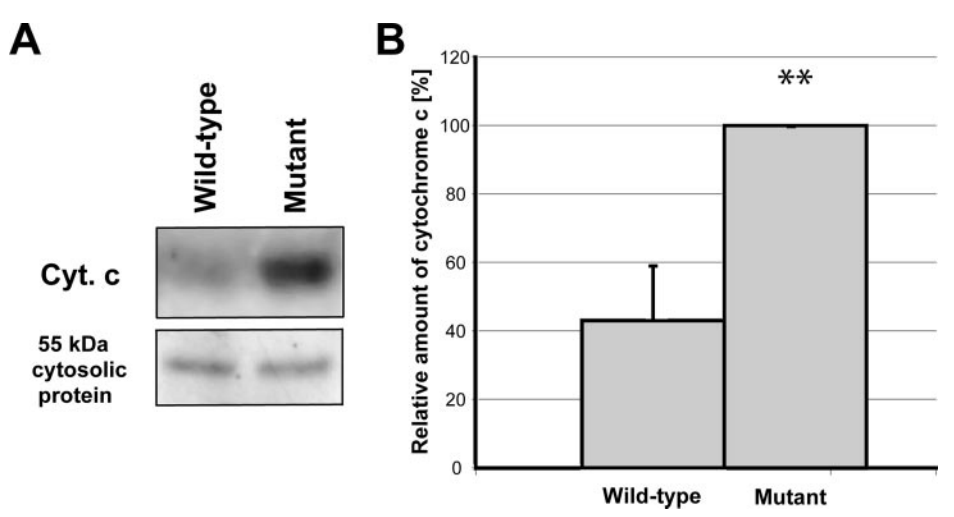


FIGURE 3. **Release of cytochrome c into the cytosol of** *cdc48*<sup>5565G</sup> **cells.** Increased amounts of cytochrome *c* were found in the cytosol in *cdc48*<sup>5565G</sup> compared with wild-type cells. *A*, representative immunoblot of cytochrome c (10  $\mu$ g of protein load per lane). The 55-kDa cytosolic protein was used as loading control. B, histogram showing levels of cytochrome c in the cytosol. Note that yeast cultures grown on (fermentative) glucose medium contain mitochondria with a certain tendency for disruption resulting in marked amounts of cytochrome c in the cytosol of wild-type strain upon cell fractionation. However, the significant higher amounts of cytochrome c levels in the cytosol of  $cdc48^{SS6SG}$  cells suggest for a pronounced higher fragility of mitochondria compared with wild-type. The level of cytochrome c in the cytosol of  $cdc48^{5565G}$  cells was set to 100% in every single experiment. A 2.3-fold increase in cytochrome c amount was observed in the cytosol of  $cdc48^{5565G}$ compared with wild-type cells (\*\*, p < 0.01, Student's t test). The data shown here are percent change values of six independent experiments. Error bars, ±S.D.

In addition to the alterations in mitochondrial proteins, we also observed enrichment of four cytoplasmic proteins, three proteins linked to the cytoskeleton, and two proteins with unknown localization (Table 1) in mitochondrial fractions of cdc48<sup>S565G</sup> cells. We observed accumulation F-actin capping protein  $\alpha$  subunit (CAPA, Fig. 2B, panel 3) and of the ARP2/3 complex 20-kDa subunit (Fig. 2B, panel 4). The ARP2/3 complex is associated with the actin cytoskeleton and is involved in mitochondrial motility in yeast (36). Accumulation of these proteins may suggest an altered mitochondrial motility in cdc48<sup>S565</sup> cells. We observed enrichment of the cytoplasmic protein O-acetylhomoserine sulfhydrolase (MET17, Fig. 2B, panel 5), a protein central for sulfur metabolism and glutathione synthesis (37). Glutathione is a known antioxidant in yeast (13, 38). Accumulation of this protein in mitochondrial extracts hints to an increased oxidative stress in  $cdc48^{S565G}$  cells (see below).

Interestingly, we found seven other proteins associated with the NE-ER network, a continuous membrane system consisting of the endoplasmic reticulum (ER) and the ER-related nuclear envelope (NE), to show altered levels in the mitochondrial fraction of the cdc48<sup>SS66SG</sup> strain (Table 1). In this context, ER luminal proteins, proteins integrated in or associated with the NE-ER membrane, and nuclear proteins are referred to as "NE-ER-associated." In fact, the majority (six of seven) were clearly enriched in mitochondrial extracts (Table 1). Most importantly, Cdc48p-S565G itself was found to be the NE-ER protein demonstrating the strongest enrichment in mitochondrial fractions of *cdc48* S565G cells compared with wild-type (*i.e.* 5.8-fold; Fig. 2B, panel 6, and Table 1). Accumulation of these NE-ERassociated proteins could be a result of the ER expansion and the dysfunction in ERAD earlier described in the cdc48<sup>S565G</sup> strain (8, 39).

In the cdc48<sup>SS6SG</sup> Strain Cytochrome c Accumulates in the Cytosol —Cytochrome c is a mitochondrial protein essential for the transfer of electrons from the cytochrome  $bc_1$ complex to the cytochrome c-oxidase complex of the respiratory chain. Depletion of cytochrome c leads to respiratory chain dysfunction and accumulation of ROS in yeast (40). It is a comparatively small (12 kDa) and basic protein (isoelectric point of 9.5) and therefore hardly analyzable by the applied 2-DE analysis. Hence, we looked for accumulation of cytochrome c in the cytosol using immunoblotting analysis. We found a 2.3-fold enrichment of cytochrome c in the cytosol of cdc48<sup>S565G</sup> cells compared with wild-type cells (Fig. 3A, immunoblots; for quantification see Fig. 3B). Accumulation of the soluble intermembrane protein cytochrome c in the cytosol, as well as

depletion of the soluble matrix proteins ARG5,6, MMF1, and cyclophilin C in mitochondrial extracts as evidenced by 2-DE analysis (Table 1), suggest that mitochondrial membranes are more fragile in  $cdc48^{S565G}$  cells than in wild-type cells possibly resulting in the release of mitochondrial proteins into the cytosol. These observed alterations at the mitochondrial molecular level obtained by 2-DE and immunoblotting analyses of cytochrome c consequently propose mitochondrial dysfunction in the cdc48<sup>S565G</sup> strain.

cdc48<sup>S565G</sup> Cells Show Respiratory Deficiency—To test for loss of mitochondrial functionality in the  $cdc48^{S565G}$  strain, we investigated the adaptability of both wild-type and  $cdc48^{\rm S565G}$ cells to conditions that challenge the respiratory capacity of their mitochondria. Only respiratory sufficient S. cerevisiae cells, in contrast to respiratory-deficient cells, form colonies on media containing a principal carbon and energy source, which is obligatory aerobic (lactate) for growth (41). Consequently, cells with respiratory incompetent mitochondria cannot metabolize lactate, *i.e.* they are unable to proliferate and do not form colonies. Therefore, a differential plating assay was conducted (41), in which proliferation on agar plates of wild-type and cdc48<sup>S565G</sup> cultures was analyzed. YPLac (lactate) plates were used as selective respiratory medium and YPGlc (glucose) plates as selective fermentative medium. Cultures were spotted on agar plates in dilution series, clockwise on six distinct sections (Fig. 4, e.g. plate 1), and the proliferation of the plated cultures was subsequently evaluated.

Cdc48<sup>S565G</sup> cells showed a markedly reduced proliferation on YPGlc compared with wild-type cells (Fig. 4, compare plates 1 and 2) demonstrating the important cellular role of Cdc48p impaired by the mutation. However, the lowest level of proliferation was found on YPLac (Fig. 4, plate 4). The almost complete absence of proliferation on YPLac (Fig. 4, compare plates

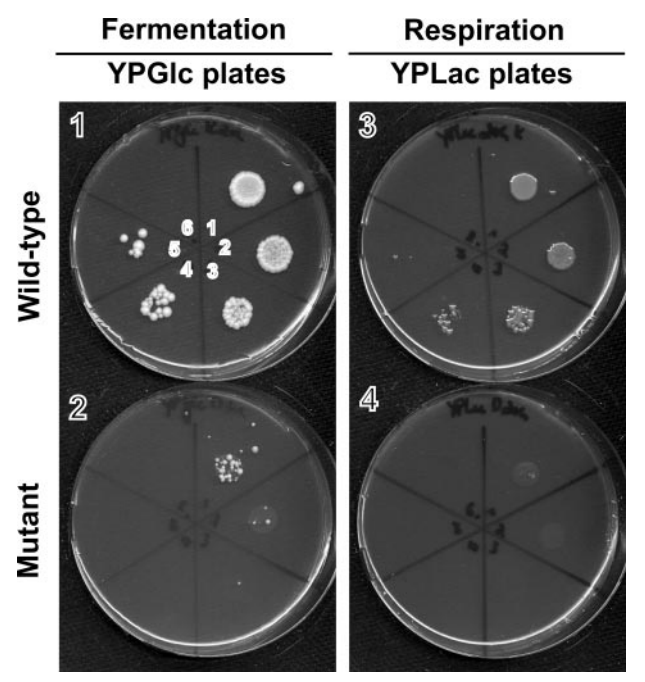
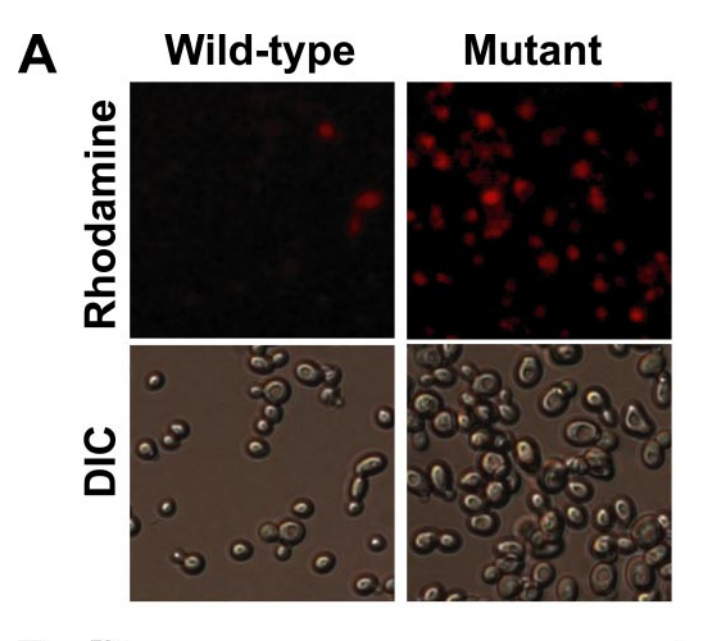


FIGURE 4. Respiratory deficiency of cdc48<sup>S565G</sup> cells. Wild-type and cdc48<sup>SS65G</sup> cultures were plated on YPLac (respiratory selective medium) and YPGIc (fermentative selective medium). Cultures were spotted on agar plates in logarithmic dilution series clockwise on six distinct sections: Section 1, 5  $\times$  $10^6$ ; section 2,  $5 \times 10^5$ ; section 3,  $5 \times 10^4$ ; section 4,  $5 \times 10^3$ ; section 5,  $5 \times 10^2$ ; and section 6,  $5\times10^1$  cells plated. Treated sections were evaluated for growth. Proliferation of  $cdc48^{SSGSG}$  cells (YPGIc) was low on YPGIc plates (plate  $\overline{2}$ ) and almost completely eliminated on YPLac plates (plate 4); n=3.

2 and 4) suggests respiratory deficiency of cdc48<sup>S565G</sup> cells probably due to their progressed state of impaired mitochondrial functionality. Such impairment was not detectable in wild-type cells under the same growth conditions (Fig. 4, compare plates 1 and 3).

Accumulating ROS in cdc48<sup>S565G</sup> Cells Are Predominantly Produced by the Mitochondrial Cytochrome bc, Complex—Mitochondrial enlargement (Fig. 1), the alterations at the mitochondrial proteome level (Fig. 2), and the observed respiratory deficiency of cdc48S565G cells (Fig. 4) suggest mitochondrial dysfunction upon CDC48 mutation. Further, the observed release of cytochrome *c* into the cytosol (Fig. 3) and the protein spot alterations of the ubiquinol-cytochrome c reductase ironsulfur subunit (UCRI, Table 1), a component of the cytochrome bc<sub>1</sub> complex of the inner mitochondrial membrane, suggest a disturbance of the respiratory chain. It is known that the cytochrome  $bc_1$  complex, upon dysfunction, is a major cellular producer of ROS (42). We therefore tested whether the emergence of ROS paralleled the observed mitochondrial impairment. In fact, we found a significantly higher number of cdc48 S565G cells (2.1-fold), which accumulated ROS compared with wild-type cells (Fig. 5A). In the cdc48<sup>S565G</sup> strain 52% of the cells were ROS-positive compared with 25% in the wild-type strain.

To show that the cytochrome  $bc_1$  complex is a major producer of ROS in the  $cdc48^{S565G}$  strain, we used myxothiazol and stigmatellin as inhibitors of this complex (42-44). Both inhibitors interrupt the electron transfer within the cytochrome  $bc_1$ complex but on two different sites (42, 43). Applying these inhibitors, we found a significant reduction in the number of cells showing ROS accumulation. In the cdc48S565G strain the



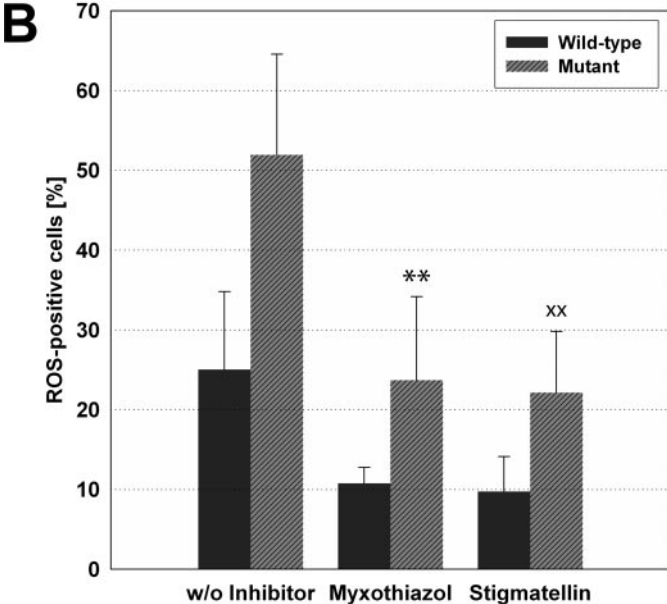
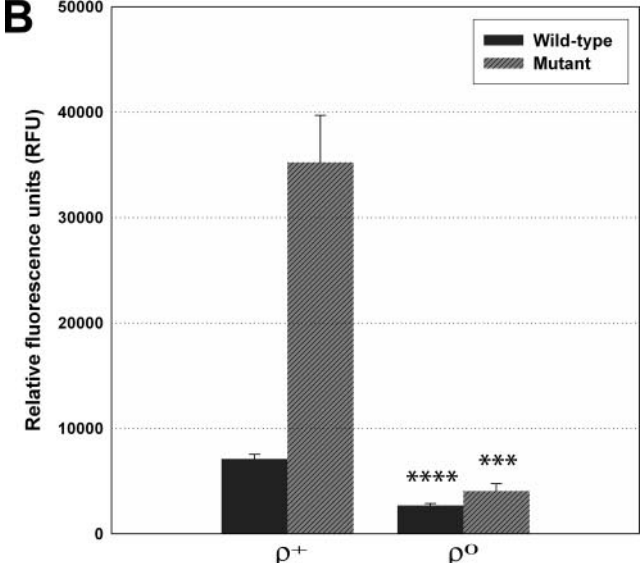
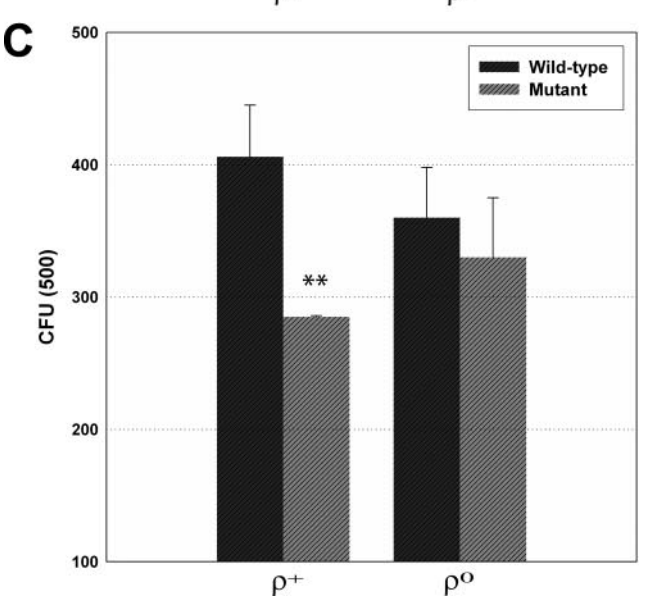


FIGURE 5. Enhanced mitochondrial ROS production in cdc48<sup>SS65G</sup> cells. A, accumulation of ROS. A significantly higher number of cdc48<sup>5565G</sup> than wildtype cells showed ROS accumulation (2.1-fold, n = 8, p < 0.002, Student's ttest). Representative micrographs of wild-type and cdc48<sup>SS6SG</sup> cells stained with dihydrorhodamine 123. For quantification >1000 cells per strain and experiment were evaluated. B, quenching of ROS accumulation. Cultures were grown in the presence of inhibitors of the cytochrome  $bc_1$  complex (myxothiazol and stigmatellin, respectively, 1 μM) and tested for accumulation of ROS (n = 4 for myxothiazol, n = 3 for stigmatellin). In the case of the  $\textit{cdc48}^{\text{S565G}} \, \text{strain, the number of ROS-accumulating cells decreased from 52\%}$ to 24% (\*\*, p < 0.005) and 22% (\*\*, p < 0.005), respectively. The number of wild-type cells showing ROS accumulation was reduced from 25% to 11% (p < 0.02) and 10% (p < 0.03), respectively. For quantification > 1000 cells per strain and experiment were evaluated. p values: Student's t test. Error bars,

proportion of ROS-positive cells was reduced from 52% to 24 and 22% for myxothiazol and stigmatellin, respectively (Fig. 5*B*). These data suggest that the mitochondrial cytochrome  $bc_1$ complex is a major site of ROS production in the cdc48<sup>S565G</sup> strain. Quenching of ROS production was also observed in the wild-type strain treated with inhibitors of the cytochrome  $bc_1$ complex. However, the significant higher number of ROS-posΑ Wild-type Mutant Rhodamine

Mitochondrial Impairment in cdc48<sup>S565G</sup> Yeast





ρ<sup>0</sup> Strains Generated from Wild-type and cdc48<sup>SS6SG</sup> Strains Show Very Low Levels of ROS Production and Highly Similar Viability-Mitochondrial contribution to the accumulation of ROS in the  $cdc48^{S565G}$  strain suggests that the observed impairment of mitochondria may lead to cellular damage. To validate such a destructive role of mitochondria, we converted the CDC48 wild-type and the  $cdc48^{S565G}$  mutant strains ( $\rho^+$ strains) into yeast strains lacking functional mitochondria ( $\rho^0$ strains). Both strains were grown overnight on media containing ethidium bromide resulting in the loss of mitochondrial DNA. Lack of mitochondrial functionality was confirmed by complete lack of growth on media containing obligatory respiratory carbon sources (glycerol).

 $\rho^0$  and  $\rho^+$  strains were evaluated for the emergence of ROS. In both  $\rho^0$  strains (wild-type and  $cdc48^{S565G}$  mutant), cells accumulating ROS were present only sporadically (Fig. 6A). Further analysis revealed a significant decrease in the production of ROS in both  $\rho^0$  strains compared with the respective  $\rho^+$ strains (Fig. 6B), i.e. 88 and 62% reduction of ROS production in  $cdc48^{S565G}$  in wild-type, respectively. These data confirm the considerable involvement of mitochondria in both wild-type and  $cdc48^{S565G}$  strains in the production of ROS as was already suggested by the decrease of ROS production via inhibition of the cytochrome  $bc_1$  complex of the respiratory chain (Fig. 5*B*). Notably, ROS production between the wild-type  $\rho^0$  and the  $cdc48^{S565G}$   $\rho^0$  strains assimilated at very low levels (Fig. 6B), further arguing that in the cdc48S565G strain impaired mitochondria are responsible for the elevated levels of ROS.

To assess the viability of both  $\rho^+$  and  $\rho^0$  cultures, we applied a survival plating assay. In this assay equal numbers of cells were plated onto YPGlc plates, and the numbers of formed colonies

FIGURE 6. Wild-type  $ho^0$  and  $cdc48^{SS65G}$   $ho^0$  strains showed very low levels of ROS production and highly similar viability. CDC48 wild-type (KFY417) and  $cdc48^{SS6SG}$  mutant (KFY437) strains ( $\rho^+$  strains) were converted into yeast strains lacking functional mitochondria ( $\rho^0$  strains) as described under "Expermental Control of the Control of imental Procedures." A,  $\rho^0$  strains are unable to accumulate ROS. Representative micrographs of wild-type  $\rho^0$  and  $cdc48^{S565G}$   $\rho^0$  cells stained with dihydroethidium. B, quantification of ROS accumulation in  $\rho^0$  and  $\rho^+$  strains. ROS accumulation was measured in a fluorescence reader after staining with dihydroethidium. In the case of the *cdc48*<sup>5565G</sup> strains, ROS accumulation was decreased by 88% in the  $\rho^0$  strain compared with the  $\rho^+$  strain (from 35,200 to 4,100 relative fluorescence units; \*\*\*, p < 0.001). ROS accumulation in the wild-type  $\rho^0$  strain was found to be reduced by 62% compared with the wildtype  $\rho^+$  strain (from 7,100 to 2,700 relative fluorescence units; \*\*\*\*, p < 0.0001). Note that ROS production in the  $cdc48^{S565G}$   $\rho^0$  and wild-type  $\rho^0$  strains assimilated at very low levels. In contrast, the  $cdc48^{S565G}$   $\rho^+$  strain showed significant higher levels of ROS compared with the wild-type  $\rho^+$ strain. The data shown here are mean values of three independent experiments. p values: Student's t test. Error bars:  $\pm$ S.D. C, cdc48<sup>S565G</sup>  $\rho^0$  strain shows highly similar viability compared with the wild-type  $\rho^0$  strain. For each culture,  $\rho^0$  and  $\rho^+$ , 500 cells were plated on YPGIc plates and the number of formed colonies (colony forming units, *CFU*) was determined. The viability of the  $cdc48^{S565G}$   $\rho^0$  strain was highly similar when compared with the wild-type  $\rho^0$  strain (8% lower viability of the  $cdc48^{S565G}$   $\rho^0$  strain compared with the wild-type  $\rho^0$  strain, p=0.42). In contrast, the  $cdc48^{S565G}$   $\rho^+$  strain revealed a signary  $\rho^+$  strain revealed as ignary  $\rho^+$ nificant decreased viability compared with the wild-type  $\rho^+$  strain (30% decrease, p < 0.01). Notably, the viability of the  $cdc48^{S565G}$   $\rho^0$  strain was found to be increased compared with the  $cdc48^{S565G}$   $\rho^+$  strain. The data shown here are mean values of three independent experiments. p values: Student's t test. *Error bars*:  $\pm$ S.D.

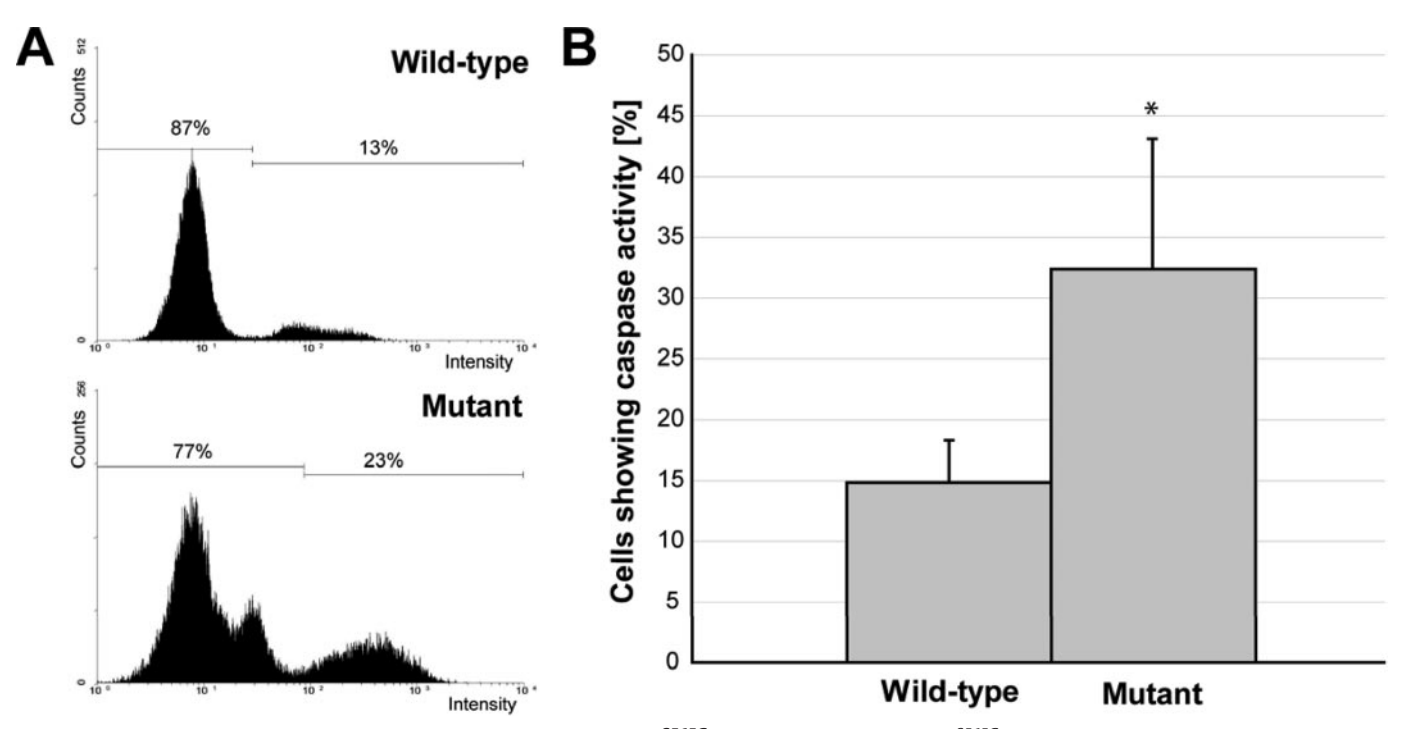


FIGURE 7. Emergence of caspase-like enzymatic activity in the cdc48<sup>S565G</sup>strain. Wild-type and cdc48<sup>S565G</sup> cells were labeled for active caspase by the cell-permeable fluorescence-labeled caspase inhibitor FITC-VAD-FMK and analyzed by flow cytometry as described under "Experimental Procedures." A, representative flow cytometric diagrams of wild-type and cdc48<sup>SS6SG</sup> strain. The nature of the second peak in the flow cytometric diagram of the cdc48<sup>SS6SG</sup> strain remained unknown. B, quantification of caspase activity. A 2.2-fold increase in caspase activity was observed in the cdc48<sup>SS6SG</sup> compared with the wild-type strain (n = 3; \*, p < 0.05; Student's t test). Error bars:  $\pm$ S.D.

were determined. The  $cdc48^{S565G} \rho^+$  strain showed a significant lower viability (30% decrease) than the wild-type  $\rho^+$  strain (Fig. 6C), as evidenced by the decreased number of formed colonies. In contrast, the viabilities of the  $cdc48^{S565G}$   $\rho^0$  and the wild-type  $\rho^0$  strains assimilated (Fig. 6C). Notably, the viability of the  $cdc48^{ ext{S565G}}\,
ho^0$  strain lacking functional mitochondria was slightly higher (16% increase) than the viability of the  $cdc48^{S565G} \rho^+$  strain. These data hint to a deleterious role of the impaired mitochondria in the mutant  $cdc48^{S565G}$  strain.

Caspase-like Enzymatic Activity and DNA Fragmentation Emerge in the cdc48<sup>SS6SG</sup> Strain—Recently, a yeast protein demonstrating caspase-like enzymatic activity upon applied oxidative stress has been described (27). Since we demonstrated accumulation of ROS (Figs. 5 and 6), we tested for caspase-like enzymatic activity in vivo in the wild-type and the cdc48<sup>S565G</sup> strains. Cells were labeled for active caspase with the fluorescence-tagged and cell-permeable caspase inhibitor FITC-VAD-FMK and analyzed by flow cytometry. A significantly higher portion of cdc48<sup>S565G</sup> than of wild-type cells (2.2-fold) demonstrated caspase-like enzymatic activity (Fig. 7A; for quantification see Fig. 7B). Using DNA fragmentation as a marker of apoptosis (TUNEL assay), consistently to previous results (8), cell death was observed in 50% of cdc48<sup>S565G</sup> cells, whereas cell death in wild-type cells did not exceed 20% (see supplemental Fig. S1A, micrographs; for quantification see supplemental Fig. S1B). Thus, the observed mitochondrial impairment due to CDC48 mutation is paralleled by the emergence of apoptotic cell death as indicated by caspase-like enzymatic activity and DNA fragmentation.

### **DISCUSSION**

Mitochondria Are Crucially Impaired in Apoptotic  $cdc48^{S565G}$  Cells—In this study we addressed the issue whether mitochondria are affected at the molecular and functional level and whether they participate in apoptosis in a yeast strain upon CDC48 mutation (cdc48S565G). Our data demonstrate mitochondrial impairment in  $cdc48^{S565G}$  cells as follows.

First, mitochondria are a specific site for qualitative as well as quantitative protein alterations in cdc48<sup>S565G</sup> cells (Fig. 2). Both "enrichment" and "depletion" of distinct proteins were seen (Table 1). In particular, we observed the depletion of two proteins, MMF1 and Ilv5p (Fig. 2), which are necessary for mitochondrial DNA stability and mitochondrial functionality (32, 33). A recent transcriptome analysis of  $cdc48^{S565G}$  cells demonstrated nuclear genes coding for mitochondrial proteins to be the largest group of differentially regulated genes (45). Thus, the observed distinct alterations at the mitochondrial protein level suggest that mitochondria are a pivotal site of changes on the protein level associated with CDC48 mutation. Second, we demonstrated mitochondrial enlargement (Fig. 1) and release of cytochrome c into the cytosol (Fig. 3) in the cdc48<sup>S565G</sup> strain compared with wild-type hinting to a facilitated mitochondrial rupture. Third, the deficit of cdc48<sup>S565G</sup> cells to adapt to respiratory growth conditions (Fig. 4) as well as accumulation of ROS produced by mitochondria (Figs. 5 and 6) suggest dysfunction of the mitochondrial respiratory chain.

Mitochondrial damage and dysfunction, release of cytochrome c into the cytosol, and emergence of ROS are characteristic features of most mitochondria-dependent apoptotic



### Mitochondrial Impairment in cdc48<sup>S565G</sup> Yeast

pathways in both mammalian cells and in yeast (17–19). Consistently to previous studies (8, 13, 45), we observed apoptotic cell death in the cdc48<sup>S565G</sup> strain as evidenced by DNA fragmentation (supplemental Fig. S1). Moreover, we revealed the emergence of caspase-like enzymatic activity in the cdc48<sup>S565G</sup> strain (Fig. 7) concomitantly to the accumulation of ROS (Fig. 5). In yeast, the caspase Yca1p is activated upon exogenously applied oxidative stress (27). Thus, it is likely that endogenously accumulating ROS in the cdc48<sup>S565G</sup> strain induce caspase activity that precedes and subsequently triggers DNA fragmentation and cell death. In a previous study, ROS have been demonstrated to be essential for the progression of cell death in the cdc48<sup>S565G</sup> strain (13). Therefore, the increased production of ROS by the mitochondrial cytochrome  $bc_1$  complex suggests a mitochondrial contribution in apoptotic cell death in the cdc48<sup>S565G</sup> strain. Consistently, generation of yeast strains lacking functional mitochondria ( $\rho^0$  strains) revealed that the  $cdc48^{S565G} \rho^0$  strain was found to be highly similar to the wildtype  $\rho^0$  strain in both cell viability (Fig. 6) and growth rates (data not shown). In contrast, the  $cdc48^{S565G} \rho^+$  strain showed significantly lower cell viability (Fig. 6) and a markedly decreased growth rate (data not shown) compared with the wild-type  $\rho^+$ strain. These data indicate that mitochondria play a detrimental role during cell death in the *cdc48*<sup>S565G</sup> strain.

Single protein spot alterations in 2-DE of mitochondrial extracts sustain mitochondrial involvement in apoptotic cell death. We found depletion of cyclophilin C in mitochondrial extracts of apoptotic yeast (Fig. 2). Mitochondrial cyclophilin in mammalian cells has been described as a repressor of mitochondria-dependent apoptosis (46). Depletion of its homologue during apoptosis suggests a similar role in yeast. We observed accumulation of the actin cytoskeleton proteins ARP2/3 complex 20-kDa subunit (Fig. 2) and F-actincapping protein  $\alpha$  subunit (CAPA, Fig. 2). Recently, a connection between yeast apoptosis and actin dynamics has been made (47, 48). These authors demonstrated that decreased actin dynamics caused depolarization of the mitochondrial membrane and an increase in ROS production resulting in cell death, highly similar features we observed in this study.

We found several proteins associated with the NE-ER to be enriched in mitochondrial extracts in the *cdc48*<sup>S565G</sup> strain (Table 1) suggesting an increased NE-ER content in mitochondrial fractions. Interestingly, the strongest accumulation was observed for Cdc48p-S565G itself (Fig. 2). Previous studies revealed deficiency of the ER-associated protein degradation (ERAD) pathway (39) and expansion of the ER (8) in the *cdc48*<sup>S565G</sup> strain. Thus, enhanced co-purification of NE-ER-associated proteins might be a result of ERAD dysfunction upon *CDC48* mutation. Notably, we found that ERAD deficiency in the *cdc48*<sup>S565G</sup> strain is paralleled with an increased co-purification of NE-ER-derived microsomes with mitochondria.<sup>4</sup> Interestingly, Haynes *et al.* have shown that, in an ERAD-deficient yeast strain, overexpression of a single misfolded

model protein leads to ER stress, accumulation of ROS, and ultimately apoptotic cell death (49). These authors demonstrated contribution of mitochondria to ROS accumulation arising from inhibition of ERAD. Thus, the mitochondrial impairment and contribution in apoptotic cell death in the  $cdc48^{\rm S565G}$  strain observed in our study might be a consequence of the described ERAD dysfunction in this strain (39).

Cdc48p/VCP-mediated Apoptosis and Human Disease—Cdc48p/VCP is a highly conserved protein essential for cellular function (for review see Ref. 4). Upon mutation impairment of Cdc48p/VCP-mediated functions increase the risk for apoptotic cell death in different species. Classic morphological apoptotic characteristics, e.g. DNA fragmentation, chromatin condensation, nuclear fragmentation, and membrane blebbing, were observed in cells expressing mutated Cdc48p/VCP homologues in mammalian cell cultures (9, 10), in trypanosomes (11), in zebrafish (12), and in budding yeast (8), although the molecular mechanisms of how impairment of Cdc48p/VCP relates to apoptotic cell death remain largely unknown. Especially mitochondrial contribution to cell death has not been demonstrated yet.

This study revealed crucial mitochondrial impairment in the *cdc48*<sup>S565G</sup> yeast strain associated with apoptosis. Yeast Cdc48p and its orthologues, such as mammalian VCP show very high sequence and functional conservation (50). Therefore, we suggest mitochondria as being involved in apoptotic cell death in other species expressing mutant variants of Cdc48p/VCP.

Mutant VCP is an inductor of IBMPFD, a dominant human disorder (5, 6). Wild-type VCP has been described as a pathological mediator for human polyglutamine diseases (7, 10, 51). In these disorders and in particular Huntington's disease, typical features of mitochondria-dependent cell death have been noted: depolarization of mitochondria, emergence of ROS, and cytochrome c release (52, 53). Thus, our finding of a mitochondrial contribution to cell death in  $cdc48^{S565G}$  yeast is compatible with the role of both Cdc48p/VCP and mitochondria in these human disorders. Based on this study we propose  $cdc48^{S565G}$  yeast as a model to elucidate the remaining unknown processes of VCP-mediated apoptosis in human degenerative diseases.

Acknowledgments—We thank Drs. C. Borner, N. Kinkl, W. Kolch, U. Olazabal, and E. E. Rojo for very helpful discussions and critical reading of the manuscript. We especially thank Dr. A. Borst for his support with EM as well as Drs. G. Blobel and F. Sherman for providing antibodies.

### **REFERENCES**

- Elkabetz, Y., Shapira, I., Rabinovich, E., and Bar-Nun, S. (2004) J. Biol. Chem. 279, 3980 – 3989
- 2. Ye, Y., Meyer, H. H., and Rapoport, T. A. (2001) Nature 414, 652-656
- 3. Richly, H., Rape, M., Braun, S., Rumpf, S., Hoege, C., and Jentsch, S. (2005) *Cell* **120**, 73–84
- 4. Woodman, P. G. (2003) J. Cell Sci. 116, 4283-4290
- Watts, G. D., Wymer, J., Kovach, M. J., Mehta, S. G., Mumm, S., Darvish, D., Pestronk, A., Whyte, M. P., and Kimonis, V. E. (2004) *Nat. Genet.* 36, 377–381
- Schroder, R., Watts, G. D., Mehta, S. G., Evert, B. O., Broich, P., Fliessbach, K., Pauls, K., Hans, V. H., Kimonis, V., and Thal, D. R. (2005) *Ann. Neurol.* 57, 457–461



<sup>&</sup>lt;sup>4</sup> H. Zischka, R. J. Braun, E. P. Marantidis, D. Büringer, C. Bornhoevd, S. M. Hauck, O. Demmer, C. J. Gloeckner, A. S. Reichert, F. Madeo, and M. Ueffing, manuscript submitted.

### Mitochondrial Impairment in cdc48<sup>S565G</sup> Yeast

- 7. Higashiyama, H., Hirose, F., Yamaguchi, M., Inoue, Y. H., Fujikake, N., Matsukage, A., and Kakizuka, A. (2002) Cell Death Differ. 9, 264-273
- 8. Madeo, F., Frohlich, E., and Frohlich, K. U. (1997) J. Cell Biol. 139, 729 - 734
- 9. Shirogane, T., Fukada, T., Muller, J. M., Shima, D. T., Hibi, M., and Hirano, T. (1999) Immunity 11, 709-719
- 10. Hirabayashi, M., Inoue, K., Tanaka, K., Nakadate, K., Ohsawa, Y., Kamei, Y., Popiel, A. H., Sinohara, A., Iwamatsu, A., Kimura, Y., Uchiyama, Y., Hori, S., and Kakizuka, A. (2001) Cell Death Differ. 8, 977-984
- 11. Lamb, J. R., Fu, V., Wirtz, E., and Bangs, J. D. (2001) J. Biol. Chem. 276,
- 12. Imamura, S., Ojima, N., and Yamashita, M. (2003) FEBS Lett. 549, 14-20
- 13. Madeo, F., Frohlich, E., Ligr, M., Grey, M., Sigrist, S. J., Wolf, D. H., and Frohlich, K. U. (1999) J. Cell Biol. 145, 757-767
- 14. Ludovico, P., Madeo, F., and Silva, M. (2005) IUBMB Life 57, 129-135
- 15. Madeo, F., Herker, E., Wissing, S., Jungwirth, H., Eisenberg, T., and Frohlich, K. U. (2004) Curr. Opin. Microbiol. 7, 655-660
- 16. Weinberger, M., Ramachandran, L., and Burhans, W. C. (2003) IUBMB *Life* **55**, 467–472
- 17. Green, D. R., and Kroemer, G. (2004) Science 305, 626-629
- 18. Ludovico, P., Rodrigues, F., Almeida, A., Silva, M. T., Barrientos, A., and Corte-Real, M. (2002) Mol. Biol. Cell 13, 2598-2606
- 19. Newmeyer, D. D., and Ferguson-Miller, S. (2003) Cell 112, 481-490
- 20. Madeo, F., Schlauer, J., and Frohlich, K. U. (1997) Gene (Amst.) 204, 145 - 151
- 21. Zischka, H., Weber, G., Weber, P. J., Posch, A., Braun, R. J., Buhringer, D., Schneider, U., Nissum, M., Meitinger, T., Ueffing, M., and Eckerskorn, C. (2003) Proteomics 3, 906-916
- 22. Byers, B., and Goetsch, L. (1991) in Guide to Yeast Genetics and Molecular Biology (Guthrie, C., ed) pp. 603-626, Academic Press, San Diego, CA
- 23. Shevchenko, A., Wilm, M., Vorm, O., and Mann, M. (1996) Anal. Chem. **68**, 850 – 858
- 24. Rabilloud, T., Strub, J. M., Luche, S., van Dorsselaer, A., and Lunardi, J. (2001) Proteomics 1, 699-704
- 25. Neuhoff, V., Arold, N., Taube, D., and Ehrhardt, W. (1988) Electrophoresis
- 26. Kussmann, M., and Roepstorff, P. (2000) Methods Mol. Biol. 146, 405-424
- 27. Madeo, F., Herker, E., Maldener, C., Wissing, S., Lachelt, S., Herlan, M., Fehr, M., Lauber, K., Sigrist, S. J., Wesselborg, S., and Frohlich, K. U. (2002) Mol. Cell 9, 911-917
- 28. Bernardi, P., Scorrano, L., Colonna, R., Petronilli, V., and Di Lisa, F. (1999) Eur. J. Biochem. 264, 687-701
- 29. Boya, P., Cohen, I., Zamzami, N., Vieira, H. L., and Kroemer, G. (2002) Cell Death Differ. 9, 465-467
- 30. Farber, J. L. (1994) Environ. Health Perspect. 102, Suppl. 10, 17-24
- 31. Wakabayashi, T. (1999) Acta Biochim. Pol. 46, 223-237
- 32. Oxelmark, E., Marchini, A., Malanchi, I., Magherini, F., Jaquet, L., Hajibagheri, M. A., Blight, K. J., Jauniaux, J. C., and Tommasino, M. (2000) Mol. Cell Biol. 20, 7784-7797

- 33. Zelenaya-Troitskaya, O., Perlman, P. S., and Butow, R. A. (1995) EMBO J. **14,** 3268 – 3276
- 34. Arevalo-Rodriguez, M., Wu, X., Hanes, S. D., and Heitman, J. (2004) Front. Biosci. 9, 2420 – 2446
- 35. Graack, H. R., and Wittmann-Liebold, B. (1998) Biochem. J. 329, 433-448
- 36. Boldogh, I. R., Yang, H. C., Nowakowski, W. D., Karmon, S. L., Hays, L. G., Yates, J. R., 3rd, and Pon, L. A. (2001) Proc. Natl. Acad. Sci. U. S. A. 98, 3162-3167
- 37. Miyake, T., Sammoto, H., Kanayama, M., Tomochika, K., Shinoda, S., and Ono, B. (1999) Yeast 15, 1449-1457
- 38. Drakulic, T., Temple, M. D., Guido, R., Jarolim, S., Breitenbach, M., Attfield, P. V., and Dawes, I. W. (2005) FEMS Yeast Res. 5, 1215-1228
- Jarosch, E., Taxis, C., Volkwein, C., Bordallo, J., Finley, D., Wolf, D. H., and Sommer, T. (2002) Nat. Cell Biol. 4, 134-139
- 40. Barros, M. H., Netto, L. E., and Kowaltowski, A. J. (2003) Free Radic. Biol. Med. 35, 179-188
- 41. Ogur, M., and St John, R. (1956) J. Bacteriol. 72, 500-504
- 42. Fang, J., and Beattie, D. S. (2003) Free Radic. Biol. Med. 34, 478 488
- 43. Crofts, A. R., Barquera, B., Gennis, R. B., Kuras, R., Guergova-Kuras, M., and Berry, E. A. (1999) Biochemistry 38, 15807-15826
- Pozniakovsky, A. I., Knorre, D. A., Markova, O. V., Hyman, A. A., Skulachev, V. P., and Severin, F. F. (2005) J. Cell Biol. 168, 257-269
- Laun, P., Ramachandran, L., Jarolim, S., Herker, E., Liang, P., Wang, J., Weinberger, M., Burhans, D. T., Suter, B., Madeo, F., Burhans, W. C., and Breitenbach, M. (2005) FEMS Yeast Res. 5, 1261-1272
- 46. Schubert, A., and Grimm, S. (2004) Cancer Res. 64, 85-93
- 47. Breitenbach, M., Laun, P., and Gimona, M. (2005) Trends Cell Biol. 15,
- 48. Gourlay, C. W., Carpp, L. N., Timpson, P., Winder, S. J., and Ayscough, K. R. (2004) J. Cell Biol. 164, 803-809
- 49. Haynes, C. M., Titus, E. A., and Cooper, A. A. (2004) Mol. Cell 15, 767–776
- 50. Frohlich, K. U., Fries, H. W., Rudiger, M., Erdmann, R., Botstein, D., and Mecke, D. (1991) J. Cell Biol. 114, 443-453
- 51. Mizuno, Y., Hori, S., Kakizuka, A., and Okamoto, K. (2003) Neurosci. Lett. **343,** 77-80
- 52. Jana, N. R., Zemskov, E. A., Wang, G., and Nukina, N. (2001) Hum. Mol. Genet. 10, 1049-1059
- 53. Wyttenbach, A., Sauvageot, O., Carmichael, J., Diaz-Latoud, C., Arrigo, A. P., and Rubinsztein, D. C. (2002) Hum. Mol. Genet. 11, 1137-1151
- 54. Sickmann, A., Reinders, J., Wagner, Y., Joppich, C., Zahedi, R., Meyer, H. E., Schonfisch, B., Perschil, I., Chacinska, A., Guiard, B., Rehling, P., Pfanner, N., and Meisinger, C. (2003) Proc. Natl. Acad. Sci. U. S. A. 100, 13207-13212
- 55. Rinnerthaler, M., Jarolim, S., Heeren, G., Palle, E., Perju, S., Klinger, H., Bogengruber, E., Madeo, F., Braun, R. J., Breitenbach-Koller, L., Breitenbach, M., and Laun, P. (2006) Biochim. Biophys. Acta 1757, 631-638
- Ruohola, H., and Ferro-Novick, S. (1987) Proc. Natl. Acad. Sci. U. S. A. 84, 8468 - 8472
- 57. Nicchitta, C. V. (2002) Curr. Opin. Cell Biol. 14, 412-416

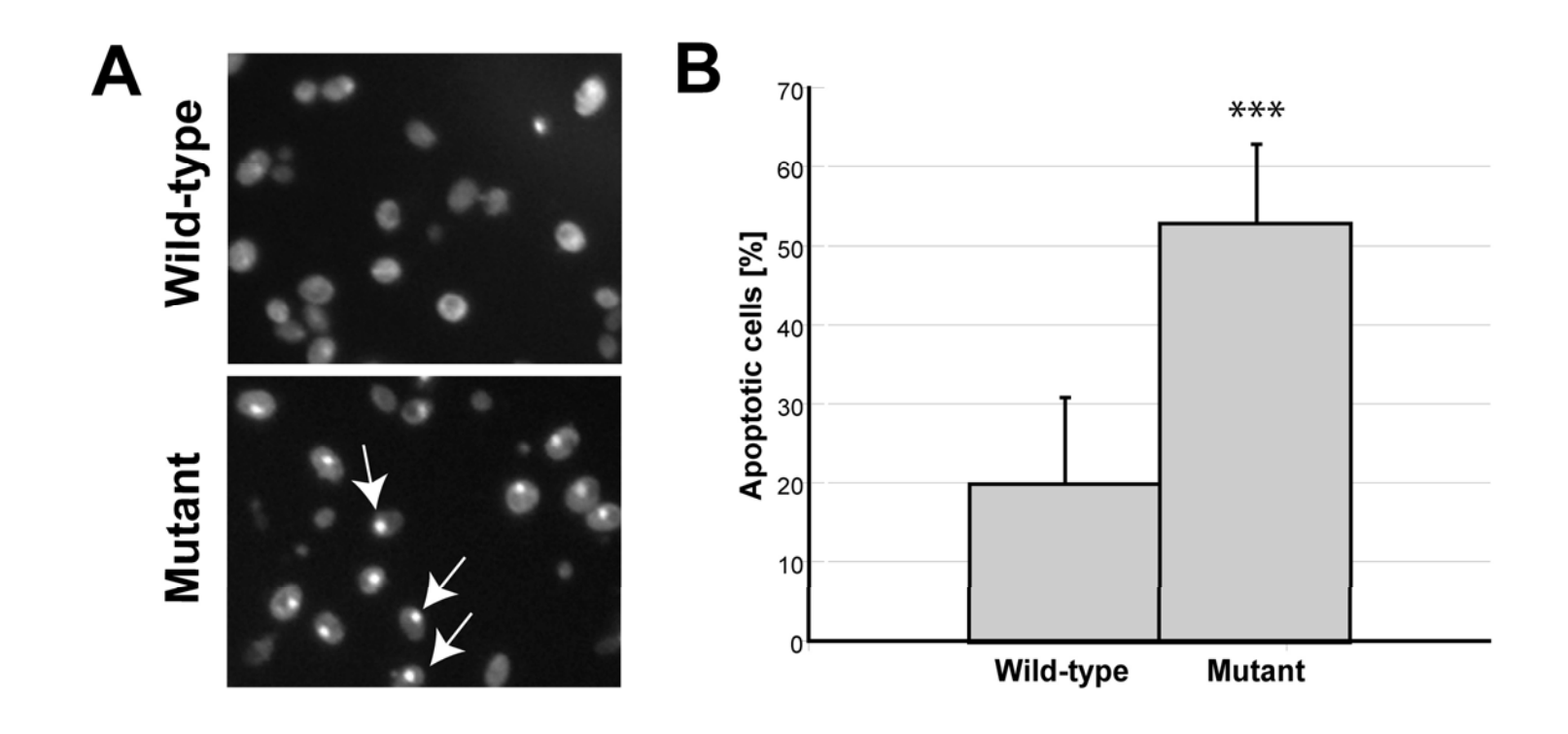


### Supplementary Figure 1:

### DNA fragmentation can be induced in cdc48S565G cells.

- (A) DNA fragmentation, visualized by TUNEL staining, is increased in *cdc48*S565G cells compared to wild-type cells. Representative micrographs of wild-type and *cdc48*S565G cells.
- (B) Quantification reveals 2.6 fold increase in *cdc48*S565G cells showing DNA fragmentation compared to wild-type cells (n=4, \*\*\*p<0.001, Student's t-test). Error bars: s.d.

# Supplementary Figure 1



### Crucial Mitochondrial Impairment upon CDC48 Mutation in Apoptotic Yeast

Ralf J. Braun, Hans Zischka, Frank Madeo, Tobias Eisenberg, Silke Wissing, Sabrina Büttner, Silvia M. Engelhardt, Dietmute Büringer and Marius Ueffing

J. Biol. Chem. 2006, 281:25757-25767. doi: 10.1074/jbc.M513699200 originally published online July 5, 2006

Access the most updated version of this article at doi: 10.1074/jbc.M513699200

### Alerts:

- When this article is cited
- · When a correction for this article is posted

Click here to choose from all of JBC's e-mail alerts

### Supplemental material:

http://www.jbc.org/content/suppl/2006/07/06/M513699200.DC1.html

This article cites 56 references, 21 of which can be accessed free at http://www.jbc.org/content/281/35/25757.full.html#ref-list-1